

## A numerical model for flood routing

S. N. KATHURIA

Meteorological Office, New Delhi

(Received 5 June 1980)

**ABSTRACT.** The paper presents an attempt to develop a numerical model for flood routing. This has been done for the river *Yamuna*. Using an implicit difference scheme, we present results to show that the model predicts the discharge and time of arrival of the peak flood with reasonable accuracy.

### 1. Introduction

Modern management of water resources requires good techniques for flood forecasting. Such techniques may be classified in two broad categories, namely, (i) hydrologic methods and (ii) hydraulic models.

Hydrological routing employs an equation for the mass balance of water and a relationship to describe the storage of the system. On the other hand, hydraulic routing is based on the equations of fluid mechanics, namely, an equation for the conservation of momentum which is coupled with the equation of continuity. Numerical solutions of these equations are now possible with computer facilities in India. As the equations are non-linear, analytical solutions are not possible.

The partial differential equations which are used in this area can be often conveniently solved by finding the characteristics of the system. Numerical integration is then possible along the characteristic equations. On some occasions, however, it is convenient to use finite difference without resorting to characteristics.

An explicit method for integration was first used by Isaacson *et al.* (1956). It was soon realised that this method had one major difficulty. This was the stability condition,  $c\Delta t/\Delta x < 1$  which imposed severe restrictions on the increments of time and space. Here we have represented the phase speed by  $c$ , the increment in time by  $\Delta t$  and the increment in space by  $\Delta x$ .

Implicit finite difference schemes permit us to use larger time increments. This has been applied for flood routing by several authors

(Baltzer and Lai 1968; Amein 1968; Amein and Fang 1970).

In this paper, the equations of unsteady flow were solved by an implicit finite difference scheme. The resulting difference equations were solved by Newton-Raphson iteration. This was applied to the river *Yamuna*. As the data that were available to us were scanty, the model was calibrated with the data available for an earlier flood (1974). Using this method of calibration, we solved the equations to predict the flood for a subsequent year (1977). The length of the river was taken to be 90 km between Kalanaur at the upstream and the Mawi at the downstream point. The course of the river is shown in Fig. 1. A flood of 96 hours duration was selected for routing. Initially, the flow rate was assumed to be the same, that is, the base flow was the same at each section. The full reach was divided into four sections each at an interval of 30 km from the other.

The discharge and time of arrival at downstream was predicted with an accuracy of 10 per cent. In spite of the limitations of scanty geometric data, the method proved to be fast, accurate and useful for routing the flood in *Yamuna*.

### 2. Symbols

The following symbols have been used :

- $A$  : Cross-section area (m<sup>2</sup>) of the channel
- $X$  : Distance (m) downstream along the channel
- $t$  : Time (sec)
- $y$  : Vertical depth of flow (m)
- $Q$  : Flow rate (cumecs)
- $q$  : Lateral inflow (cumecs)

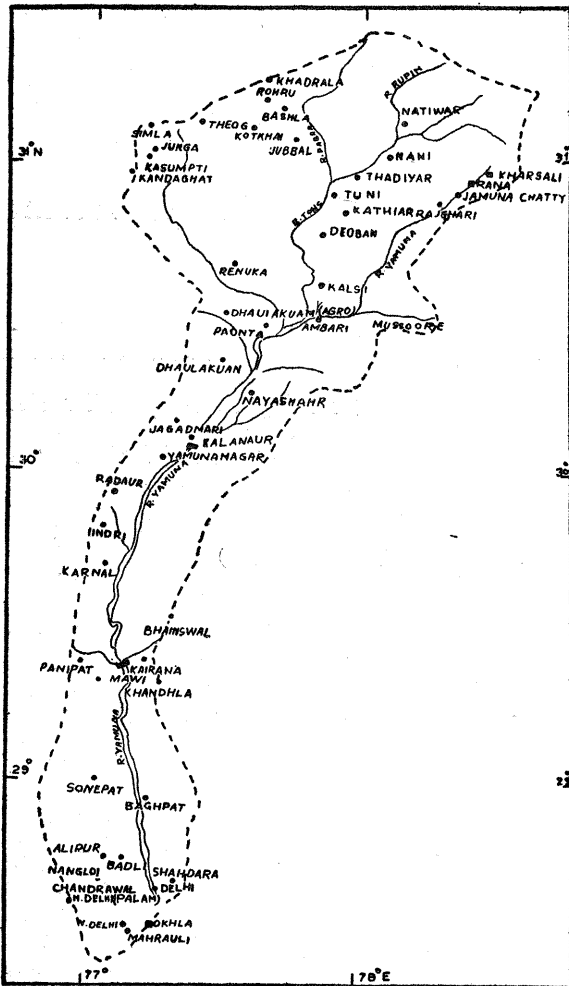


Fig. 1. Base map of Yamuna river up to Delhi

- Z : bottom elevation (m)
- g : acceleration due to gravity (m sec<sup>-2</sup>)
- S<sub>0</sub> : channel bottom slope
- S<sub>f</sub> : frictional slope

We define the frictional slope by

$$S_f = n^2 Q^2 B^{4/3} / A^{10/3} \quad (2.1)$$

where *n* is Manning's roughness coefficient and *B* is the wetted perimeter of the flowing stream. We have

$$B = 2y + b \quad (2.2)$$

where *b* represents the width of the flowing stream (m).

The cross-sectional area (*A*) of the moving stream is taken to be the same for the whole river. It is

$$A = a_1 + a_2 y a_3 \quad (2.3)$$

where *a*<sub>1</sub>, *a*<sub>2</sub>, *a*<sub>3</sub> are constants depending on the geometry of the river. They are pre-determined at every section.

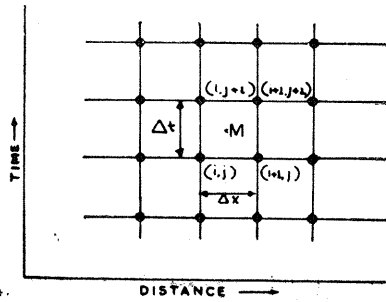


Fig. 2. The grid in the (x, t) plane

### 3. Basic equations

We represent the conservation of mass and momentum (Stoker 1957, Chow 1959) by

$$\frac{\partial A}{\partial t} + \frac{\partial Q}{\partial x} = q \quad (3.1)$$

$$\frac{\partial Q}{\partial t} + \frac{\partial}{\partial x} (Q^2/A) + gA \frac{\partial}{\partial x} (y+z) + gA S_f = 0 \quad (3.2)$$

The above equations are supplemented by one initial condition and two boundary conditions.

The initial conditions are the specified values of *y* and *Q* at *x*=0 (upstream) and *t*=0, that is, before the rise of the river stage. The boundary conditions are :

- (i) The values of *y* as a function of time at the upstream end and
- (ii) the rating curve at downstream end.

Eqns. (3.1) and (3.2) are represented by finite differences by grids in the *x-t* plane. This is shown in Fig. 2. Each discrete grid point is designated by a double subscript (*i, j*) where *i* is the *x*-position and *j* is the time level.

Let us define the following space (*i*) and time (*j*) increments for any dependent variable (*F*)

$$\delta_i F = \frac{1}{\Delta x} [F_{i+1} - F_i] \quad (3.3)$$

$$\delta_j F = \frac{1}{\Delta t} [F_{j+1} - F_j] \quad (3.4)$$

The above expressions represent forward differences of *F* in space (*i*) and time (*j*). We represent the average values of the forward differences by

$$\hat{\delta}_i F = \frac{1}{2} [(\delta_i F)_{j+1} + (\delta_i F)_j] \quad (3.5)$$

$$\hat{\delta}_j F = \frac{1}{2} [(\delta_j F)_{i+1} + (\delta_j F)_i] \quad (3.6)$$

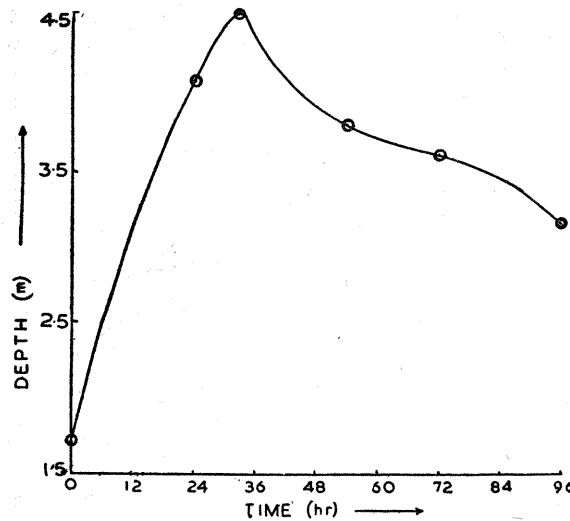


Fig. 3. Upstream boundary condition showing the growth of depth ( $y$ ) with time ( $t$ )  
 Ⓞ — denote observed data

A similar expression follows for the average value of  $F$ , namely,

$$\bar{F} = \frac{1}{4} \left[ F(i, j) + F(i+1, j) + F(i, j+1) + F(i+1, j+1) \right] \quad (3.7)$$

With the above notation, the finite difference analogues of (3.1), (3.2) with the help of (3.3)—(3.7) are

$$\delta_x Q + \delta_y A - q_i = 0 \quad (3.8)$$

$$\delta_x Q + \delta_x (Q^2/A) + g \left[ \Delta (\delta_x y + \delta_x z) \right] + g (\Delta \times \hat{S}_f) = 0. \quad (3.9)$$

Eqns. (3.8) and (3.9) form a set of two non-linear equations for  $y$  and the discharge  $Q$  at  $(i, j+1)$  and  $(i+1, j+1)$ . The values of  $y$  and  $Q$  at  $(i, j)$  and  $(i+1, j)$  are known by the initial condition or by the previous time step. For  $N$  grid points, this forms a set of  $2(N-1)$  equations. These equations are supplemented by two boundary conditions. Closed system of  $2N$  linear equations is thus obtained which we solve by the Newton's iteration.

The computation proceeds by advancing the solutions stepwise in an upstream direction. The solution of the set of equations will provide values of  $y_i$  and  $Q_j$  at the  $K$ th iteration. The

procedure can be repeated to achieve the required accuracy for the depth and discharge. The values of the variables thus obtained are at  $(j+1)$ th time step, which can be advanced to further time steps.

#### 4. Results for the Yamuna

This method was applied to route the flood in *Yamuna*. Fig. 1 depicts the base map of *Yamuna* river upto Delhi. From the map we find that there is no major tributary downstream of Kalanaur. As the present study does not include the effect of discharge from tributaries, we apply the model to the 90 km stretch from Kalanaur to Mawi.

The upstream boundary condition is given by the hydrograph at Kalanaur. The downstream boundary condition is controlled by the rating curve of Mawi, which is approximated by

$$Q = \alpha + \beta y^\gamma \quad (4.1)$$

where the constants  $\alpha$ ,  $\beta$  and  $\gamma$  are determined from the rating curve.

The computations for depth and discharge were carried out for a 3-hour time interval. From the stability condition, we find that space increment should be more than the distance travelled by flood wave in a single time increment (3-hour), that is, 21 km. Therefore, the channel reach was divided into four segments each of 30 km length.

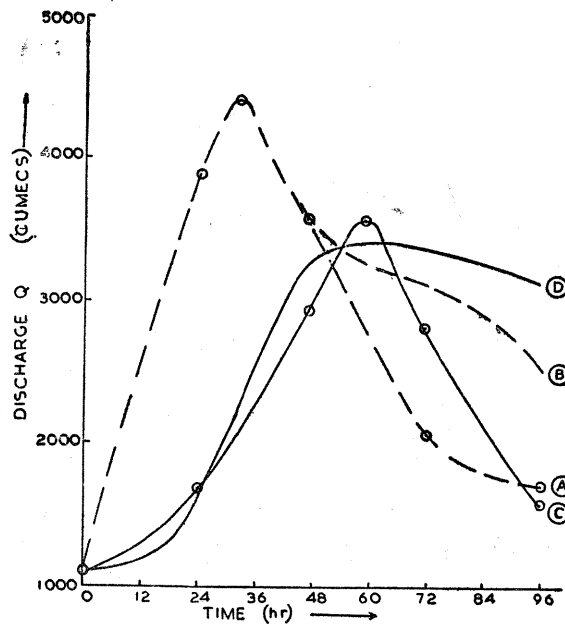


Fig. 4. Discharge hydrographs  
 (A) Observed and (B) Computed at Kalanaur  
 (C) Observed and (D) Computed at Mawi  
 ○—denote observed data

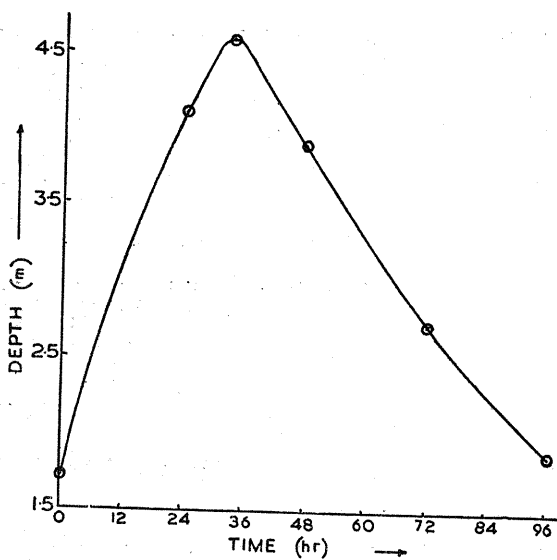


Fig. 5. Corrected upstream boundary condition showing growth of depth with time.  
 ○—denote observed data

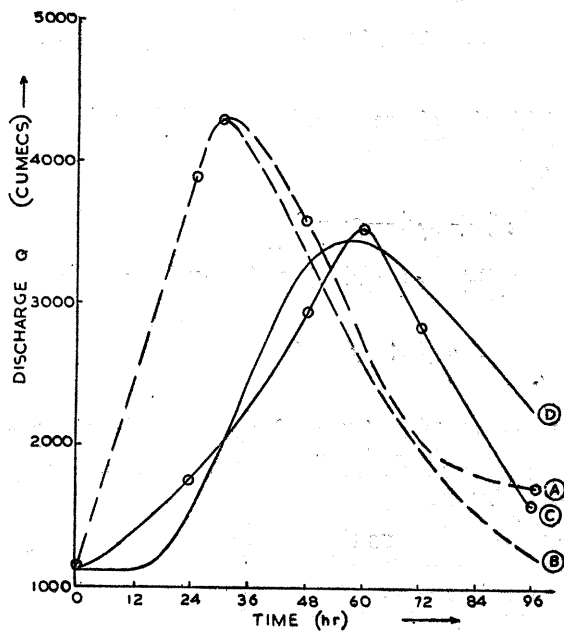


Fig. 6. Discharge hydrographs using corrected upstream boundary condition  
 (A) Observed and (B) Computed at Kalanaur  
 (C) Observed and (D) Computed at Mawi  
 ○—denote observed data

The channel cross-section area ( $A$ ) was expressed as a function of the channel depth ( $y$ ) by equation (2.3). The constants were determined by fitting the data of  $A$  and  $y$  at a section. The channel top width, ( $B$ ) is  $\partial A / \partial y$ . The wetted perimeter was equal to the top width. Manning's roughness coefficient was estimated to be 0.03.

The data were scanty. For the initial condition, the model requires the depth, discharge and velocity at all the four segments in the reach. But, the data were available only at upstream and downstream sections. The values of these parameters at 30 km and 60 km segments were computed by calibrating the model with the observed flood peak on an earlier occasion in 1974.

The upstream boundary condition requires an estimate of the growth of depth with time at an interval of 3 hours. But, the data were available only at an interval of 24 hours. To overcome this difficulty, the data were interpolated at intervals of 3 hours. This was achieved by Lagrange's interpolation. The upstream boundary condition is shown in Fig. 3.

After calibrating the model with the 1974 flood peak, the 1977 flood peak and time lag at the downstream section was forecast. The initial time corresponds to 3 August 1977 at 0830 IST. The initial upstream discharge was 1131 cumecs, with an initial depth of 1.71 m.

The convergence of the discharge computation was obtained with an error of 1 cumec, and for depth with an error of 0.01 m. The above convergence was achieved with 4 iterations. The computer time for forecasting flood for 4 days was about 3 minutes. The results of the computation are depicted in Fig. 4. The observed discharge hydrographs at upstream and downstream sections are shown as curves (A) and (C). The curves (B) and (D) are the corresponding computed hydrographs.

From Figs. 3 and 4(A), we find that the observed depths do not agree with discharge data. The difference between the two may be attributed to discrepancies in the observed depth data. The depth hydrograph was corrected so that it agrees better in amplitude with the discharge hydrograph. The data on discharges were more reliable than the observation of depth. Hence, it was considered more reasonable to apply small corrections to the observed values of depth, so that both the depth and discharge hydrographs were in reasonable agreement. The corrected depth hydrograph, which was the upstream boundary condition, is shown in Fig. 5. Using this as a

boundary condition, the flood hydrographs were computed again. They are depicted in Fig. 6. It is seen from this figure that the agreement between the computed and observed hydrographs is much better.

### 5. Summary and conclusions

As we can see from Fig. 6, the observed and computed discharge hydrographs are in good agreement. The computed discharge and time lag at the downstream section are approximately 10 per cent less than the observed values.

It may be noted that in the present study we find that the assumption of taking the slope at a section as being equal to the gradient of elevation with distance is not valid. One must take the actual slope into consideration for forecasting the time lag otherwise, the results will not be satisfactory.

It is worthwhile to mention that there is a singular point upstream of Mawi (Fig. 1). The present study is valid for a rectangular channel. Consequently, the model was calibrated after removing the singular point. The calibration of the model showed that the speed of flow decreases to 1/3 rd of its original speed after crossing the singular point.

The present study can be extended to include the effect of tributaries and contribution of runoff due to rainfall and flood forecast may be done with better accuracy.

It may be concluded that the implicit technique of flood routing may be applied to Indian rivers and flood can be forecasted with reasonable accuracy. However, better accuracy may be attained, if at least data before and after the singular points are also available besides at upstream and downstream sections.

### Acknowledgements

The author would like to thank Drs. P.K. Das and D.V.L.N. Rao for many useful discussions on this problem. He also thanks Shri R.K. Datta for his kind help in programming the model. Thanks are due to Miss Sharda Sharma for efficiently typing the manuscript.

## References

- Amein, M., 1968, An implicit method for numerical flood routing, *Water resor. Res.*, 4(4), 719-726.
- Amein, M. and Frang, C.S., 1970, Implicit flood routing in natural channels, *J. Hydraul. Div.*, Amer. Soc. Civil Eng., 96 (Hy. 12), 2481-2500.
- Baltzer, R.A. and Lai, C., 1968, computer simulation of upsteady flows in water ways, *J. Hydraul. Div.*, Amer. Soc. Civil Eng; 94 (Hy. 4 ), 1083-1117.
- Chow, V.T., 1959, *Open-channel Hydraulics*, McGraw Hill, New York.
- Isaacson, E., Stoker, J.J. and Troesch, A., 1956, Numerical solution of flood prediction and river regulation problems, Rep. IMM 2.5, Inst for Math. and Mech., New York University, New York.
- Stoker, J.J., 1957, *Water waves*, Interscience Publishers, New York.
-